Solar Energy Materials & Solar Cells 210 (2020) 110502

Contents lists available at ScienceDirect

Solar Energy Materials and Solar Cells

journal homepage: http://www.elsevier.com/locate/solmat

Impact of Urbach energy on open-circuit voltage deficit of thin-film solar cells

Jakapan Chantana [a,b,*], Yu Kawano [a], Takahito Nishimura [c], Abdurashid Mavlonov [b], Takashi Minemoto [a,**]

[a] Department of Electrical and Electronic Engineering, Ritsumeikan University, Kusatsu, Shiga, 525-8577, Japan
[b] Research Organization of Science and Technology, Ritsumeikan University, 1-1-1 Nojihigashi, Kusatsu, Shiga, 525-8577, Japan
[c] Ritsumeikan Global Innovation Research Organization, Ritsumeikan University, 1-1-1 Nojihigashi, Kusatsu, Shiga, 525-8577, Japan

ARTICLE INFO

Keywords:
Thin film
Solar cell
Urbach energy
Open-circuit voltage deficit

ABSTRACT

Correlation between Urbach energy (E_U) and open-circuit voltage deficit ($V_{OC,def}$) among conventional as well as emerging thin-film solar cells, i.e. $Cu(In,Ga)Se_2$ (CIGSe), $Cu(In,Ga)(S,Se)_2$ (CIGSSe), Cu_2SnS_3 (CTS), $Cu_2Sn_{1-x}Ge_xS_3$ (CTGS), SnS, $Cu_2ZnSnS_xSe_{4-x}$ (CZTSSe), perovskite (PVK), $Cu(In,Ga)S_2$ (CIGS), and CdTe thin-film solar cells, is examined. The E_U is estimated from an exponential tail in a long-wavelength edge of an external quantum efficiency. It is determined that the relation between short-circuit current density (J_{SC}) and E_U is not clearly shown because the J_{SC} is primarily influenced by the bandgap of the thin-film absorbers. On the other hand, E_U demonstrates a close relation with $V_{OC,def}$, where the reduction of the E_U leads to the decrease in the $V_{OC,def}$, implying that the E_U can be used as an indicator of the absorber quality. The E_U of over 20 meV, observed in the CIGS, CTS, CTGS, SnS, and CZTSSe solar cells, gives rise to the high $V_{OC,def}$ and the low conversion efficiency (η) values. The E_U of below 20 meV, seen in the CIGSe, CIGSSe, PVK, and CdTe solar cells, leads to the low $V_{OC,def}$ and high η values. Ultimately, the thin-film absorbers with the E_U values of below 20 meV, which is lower than thermal energy under room temperature, is of vital to realize high photovoltaic performances.

1. Introduction

Thin-film-based photovoltaic (PV) modules are in the rapid progress because they can be fabricated on flexible substrates for their lightweight, thereby allowing the employment of a roll-to-roll process for the cost reduction [1,2]. In thin-film solar cells, the conversion efficiencies (η) of $Cu(In,Ga)Se_2$ (CIGSe), $Cu(In,Ga)(Se,S)_2$ (CIGSSe), CdTe, and perovskite (PVK) solar cells have been significantly improved. The highest η values of the CIGSe and CIGSSe solar cells are 22.6% and 23.35%, respectively [3–5]. The record η values of the CdTe and perovskite solar cells are 22.1% and 24.2%, respectively [5,6]. Pure-sulfide $Cu(In,Ga)S_2$ (CIGS) thin-film solar cell with the bandgap (E_g) of its absorber from 1.5 to 2.43 eV under changed Ga content can be applied as a top cell for tandem solar cell with the low-cost mass production [7–9]. The highest η values of the CIGS solar cell are 15.5% for a designated area and 16.9% for an aperture area [9,10]. Since In element is a rare material, possibly making it difficult to meet the increasing demand of the PV market worldwide, and Cd element is toxic, the eco-friendly thin-film solar cells using earth-abundant and Cd-free elements for absorbers such as $Cu_2ZnSnS_xSe_{4-x}$ (CZTSSe), Cu_2SnS_3 (CTS), $Cu_2Sn_{1-x}Ge_xS_3$ (CTGS), and SnS are intriguing and intensively studied. The record η values are 12.6% for the CZTSSe solar cell [11], 6.7% for CTGS solar cell [12], 5.1% for CTS solar cell [13], and 4.36% for SnS solar cell [14], which are much lower than those of the CIGSe, CIGSSe, CdTe, and PVK solar cells. To achieve the high η of the eco-friendly thin-film solar cells with earth-abundant elements, the understanding of their physical absorber properties is of importance. The physical properties of the thin-film absorber among the thin-film solar cells are scrutinized.

The sub-gap (tail) absorption in semiconductors gives rise to the transitions between Urbach tails, which are characterized by Urbach energy (E_U) [15–17], where the Urbach tails are the state distribution with the density exponentially enhancing to the band edge. The E_U of the absorbers of thin-film solar cells can be estimated from both their

* Corresponding author. Department of Electrical and Electronic Engineering, Ritsumeikan University, Kusatsu, Shiga, 525-8577, Japan.
** Corresponding author.
E-mail addresses: jakapan@fc.ritsumei.ac.jp (J. Chantana), kawano@fc.ritsumei.ac.jp (Y. Kawano), nishi-tk@fc.ritsumei.ac.jp (T. Nishimura), mavlonov@fc.ritsumei.ac.jp (A. Mavlonov), minemoto@se.ritsumei.ac.jp (T. Minemoto).

https://doi.org/10.1016/j.solmat.2020.110502
Received 7 January 2020; Received in revised form 24 February 2020; Accepted 6 March 2020
Available online 11 March 2020

internal quantum efficiency (IQE) and external quantum efficiency (EQE) in the long-wavelength edge [15–19]. It is known that the E_U has the influence on the carrier mobility and lifetime, affecting cell performances [1,20,21], and open-circuit deficit ($V_{OC,def}$) of thin-film solar cells [22,23]. The $V_{OC,def}$ is determined by E_g/q - V_{OC}, and managed by the carrier recombination and the absorber quality [22,23]. The q and V_{OC} are elementary charge and open-circuit voltage, respectively. Some literatures have pointed out that the tail absorption strongly decreases the V_{OC}, which is attributable to the increase in the saturation current density (J_0) [24–26]. The E_U is therefore considered as one of the intriguing physical properties of the thin-film absorber and should show the relations with the PV performances and $V_{OC,def}$.

In this work, the E_U values of the different types of thin-film solar cells were mainly calculated based on their EQE. The correlations of the E_U values with the PV performances and $V_{OC,def}$ were experimentally scrutinized and compared among the different types of thin-film solar cells. With the comprehension of the correlations and the quantitative number of the E_U values, it is very useful for the future development for thin-film solar cells, especially the eco-friendly thin-film solar cells with earth-abundant elements.

2. Experimental procedure

In this work, the CTS, CTGS, and SnS thin-film solar cells on soda-lime glass (SLG) substrates, which are promising as the eco-friendly thin-film solar cells with earth-abundant elements, were primarily fabricated with a designated area of approximately 0.3 cm^2, which was investigated by microscope system (Ver. 1270, Microadvance). For the fabrication of the CTS and CTGS thin films, the 1000-nm-thick Mo layers were deposited on clean SLG substrates using sputtering process. The stacked precursors of the Cu–SnS_2 layer for the CTS thin films and the stacked precursors of the Cu–SnS_2/Ge layers for the CTGS thin films were then prepared. The Cu–SnS_2 precursors were deposited under room temperature by the co-sputtering process utilizing the 99.99%-purity Cu target and 99.5%-purity SnS_2 target. The working pressure under Ar atmosphere was 2×10^{-1} Pa. The Ge precursors were deposited by electron beam (EB) deposition method utilizing 99.99%-purity Ge grain. After preparing the stacked precursors, the sulfurization was performed on the stacked precursors of the Cu–SnS_2 layer to form the CTS thin films and on the stacked precursors of the Cu–SnS_2/Ge layers to form the CTGS thin films, respectively. The sulfurization was conducted under S and SnS_2 vapors with the N_2 flow rate of 100 ml/min for 60 min under substrate temperature (T_{sub}) of 550 °C. The detailed sulfurization process was discussed in Ref. [13]. For the deposition of the SnS thin films, they were deposited on Mo-coated SLG substrates by thermal evaporation method utilizing SnS powder with 99.9% purity as a material source. The wool fiber of SiO_2 was added in the crucible with SnS powder to suppress splashed SnS grain on the absorber surface. The detailed process was discussed in Ref. [27].

After depositing the CTS, CTGS, and SnS thin films (absorbers) on Mo-coated SLG substrates, their solar cells were next prepared with the structure of SLG/Mo/CTS, CTGS, or SnS absorber/CdS/ZnO/ZnO:Al (AZO). In the fabrication process of the thin-film solar cells, the CdS buffers with a thickness of approximately 50 nm were grown on the absorbers utilizing chemical bath deposition under a bath temperature of 80 °C. The window layers (or the second buffers) of ZnO with a thickness of about 50 nm and transparent conductive oxides (TCO) layers of AZO with a thickness of around 400 nm were deposited by the sputtering under room temperature. 99.99% purity ZnO and 99.99% purity ZnO–Al_2O_3 (2 wt%) were utilized as material targets, respectively. The bilayers of 1-μm-thick Al/50-nm-thick Ni grids were deposited by EB evaporation on both TCO layers and Mo layers for the finished solar cells. The PV performances, which are short-circuit current density (J_{SC}), V_{OC}, fill factor (*FF*), and η, were measured under standard test condition (equivalent Air Mass 1.5G illumination (100 mW/cm^2) under 25 °C) (CEP-25RR Bunkoukeiki). The external quantum efficiency (EQE) of the solar cells was observed using CEP-25RR Bunkoukeiki. The E_g values of the absorbers of the thin-film solar cells were then estimated from the first EQE derivative [13,22]. The $V_{OC,def}$ was calculated by $V_{OC,def} = E_g$/q - V_{OC}. Moreover, the E_U values of the absorbers in the thin-film solar cells were calculated from the exponential absorption tail in the long-wavelength edge of their EQE (near band edge) [18]. Under the almost constant reflectance of the solar cells, EQE in the long-wavelength edge can be expressed as follow [18];

$$\ln(EQE) = c + \frac{h\upsilon}{E_U} \quad (1)$$

where c and $h\upsilon$ are a constant and photon energy, respectively. According to Equation (1), an inverse slope between ln(EQE) in the long-wavelength edge and $h\upsilon$ results in the calculation of the E_U. For the high precision of the E_U estimation in this work, the correlation coefficient of experimental data and fitted line based on Equation (1) is over 0.95 or close to unity. The correlations of the E_U values with the PV performances and $V_{OC,def}$ were examined and compared among the different types of thin-film solar cells.

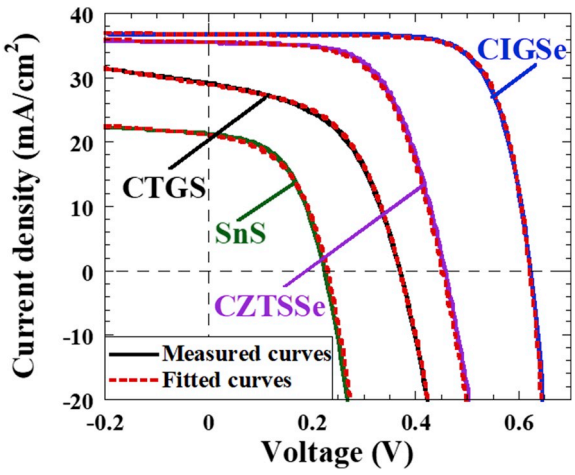

Fig. 1. Photo-*J-V* characteristics of the CIGSe, CZTSSe, CTGS, and SnS thin-film solar cells. The *J-V* characteristics of the CIGSe and CZTSSe solar cells were obtained from Refs. [28,29]. The photo-*J-V* characteristics were fitted using Lambert-W function as shown by fitted curves for the estimation of the diode parameters in Table 1.

3. Results and discussion

3.1. Comparison of PV performances among different types of thin-film solar cells

The PV performances among different types of thin-film solar cells, which are the CIGSe, CZTSSe, CTGS, and SnS thin-film solar cells, were investigated. Fig. 1 shows photo-current density-voltage (*J-V*) characteristics of the CIGSe, CZTSSe, CTGS, and SnS thin-films solar cells. The *J-V* characteristics of the CIGSe and CZTSSe solar cells were obtained from Refs. [28,29], where the photo-*J-V* characteristics were fitted using Lambert-W function as shown by fitted curves for the estimation of the diode parameters. The corresponding photovoltaic performances and diode parameters are shown in Table 1. Fig. 2 depicts the corresponding EQE spectra and (b) first EQE derivative of the CIGSe, CZTSSe, CTGS, and SnS thin-films solar cells, where Fig. 2(b) leads to the calculation of the E_g of the absorbers and the $V_{OC,def}$, as demonstrated in Table 1. It is determined that the highest η of 17.3% and the second highest η of 9.9% are shown for the CIGSe and CZTSSe solar cells, respectively. The relatively low η values of 5.4% for the CTGS solar cell and 2.4% for the SnS solar cell are obtained. This occurs because all PV performance parameters (J_{SC}, V_{OC}, and *FF*) are the highest for the CIGSe solar cell in Table 1.

Table 1
PV performances, E_g, $V_{OC,def}$, and E_U of the CIGSe, CZTSSe, CTGS, and SnS thin-film solar cells in Fig. 1. The *J-V* characteristics of the CIGSe and CZTSSe solar cells were obtained from Refs. [28,29]. The diode parameters of the solar cells such as series resistance (R_S), shunt resistance (R_{SH}), J_0, and ideality factor (n) were obtained by the curve fitting of their *J-V* characteristics using Lambert-W function.

Absorber	J_{SC} (mA/cm^2)	V_{OC} (V)	*FF* (%)	η (%)	E_U (meV)	E_g (eV)	$V_{OC,def}$ (V)	n	J_0 (A/cm^2)	R_S (Ω.cm^2)	R_{SH} (Ω.cm^2)
CIGSe [28]	36.8	0.628	74.9	17.3	14	1.05	0.422	1.65	1.73×10^{-8}	0.26	1150
CZTSSe [29]	35.6	0.456	61.0	9.9	22	1.10	0.644	1.77	1.80×10^{-6}	1.22	500
CTGS	29.1	0.370	50.5	5.4	29	1.15	0.780	1.88	1.21×10^{-5}	1.32	80
SnS	21.2	0.223	50.6	2.4	33	1.30	1.070	1.92	2.01×10^{-4}	0.52	170

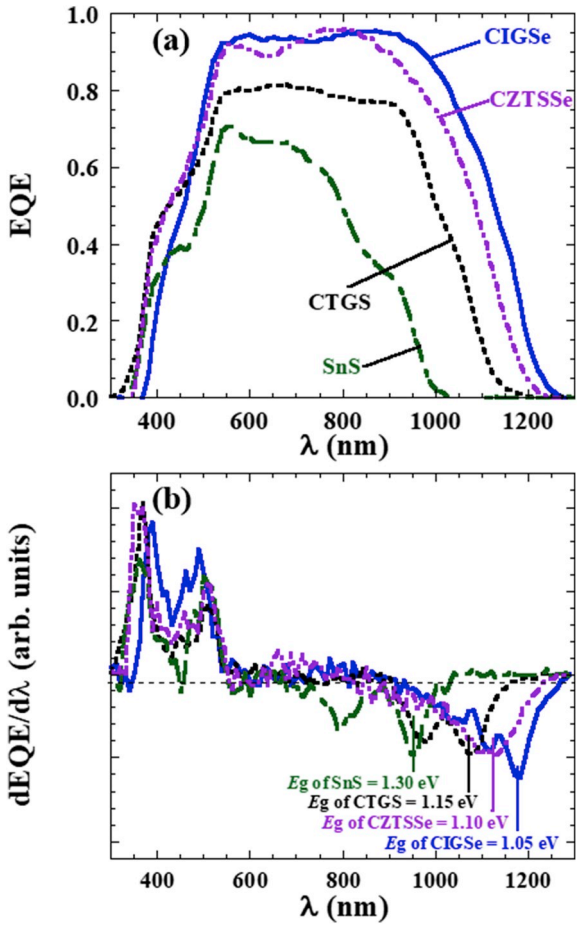

Fig. 2. (a) Corresponding EQE spectra and (b) first EQE derivative of the CIGSe, CZTSSe, CTGS, and SnS thin-films solar cells. The results of the CIGSe and CZTSSe solar cells were obtained from Refs. [28,29]. The λ presents the wavelength.

The highest J_{SC} of the CIGSe solar cell and the second highest J_{SC} of the CZTSSe solar cell are attributable to the lowest E_g of 1.05 eV for the CIGSe absorber and the second lowest E_g of 1.10 eV for the CZTSSe absorber in Table 1, thereby giving rise to their large EQE in Fig. 2(a), respectively. On the other hand, the low J_{SC} values of the CTGS and SnS solar cells are caused by the high E_g values especially in a case of SnS (E_g of 1.3 eV), thus resulting in their EQE spectra smaller than those of the CIGSe and CZTSSe solar cells. Namely, the J_{SC} of the thin-film solar cell is primarily influenced by the E_g of its absorber.

The V_{OC} and *FF* of the CIGSe solar cell are the highest, whereas those of the CTGS and SnS solar cells are the two lowest ones. The $V_{OC,def}$ of the CIGSe solar cell is furthermore observed to exclude the effect of the E_g of the CIGSe absorber in the V_{OC} parameter, and it is the lowest at 0.422 V, while the $V_{OC,def}$ values of the CTGS and SnS solar cells are the two highest values. One of the explanations of these results is the different qualities of the thin-film absorbers, which can be interpreted by the J_0

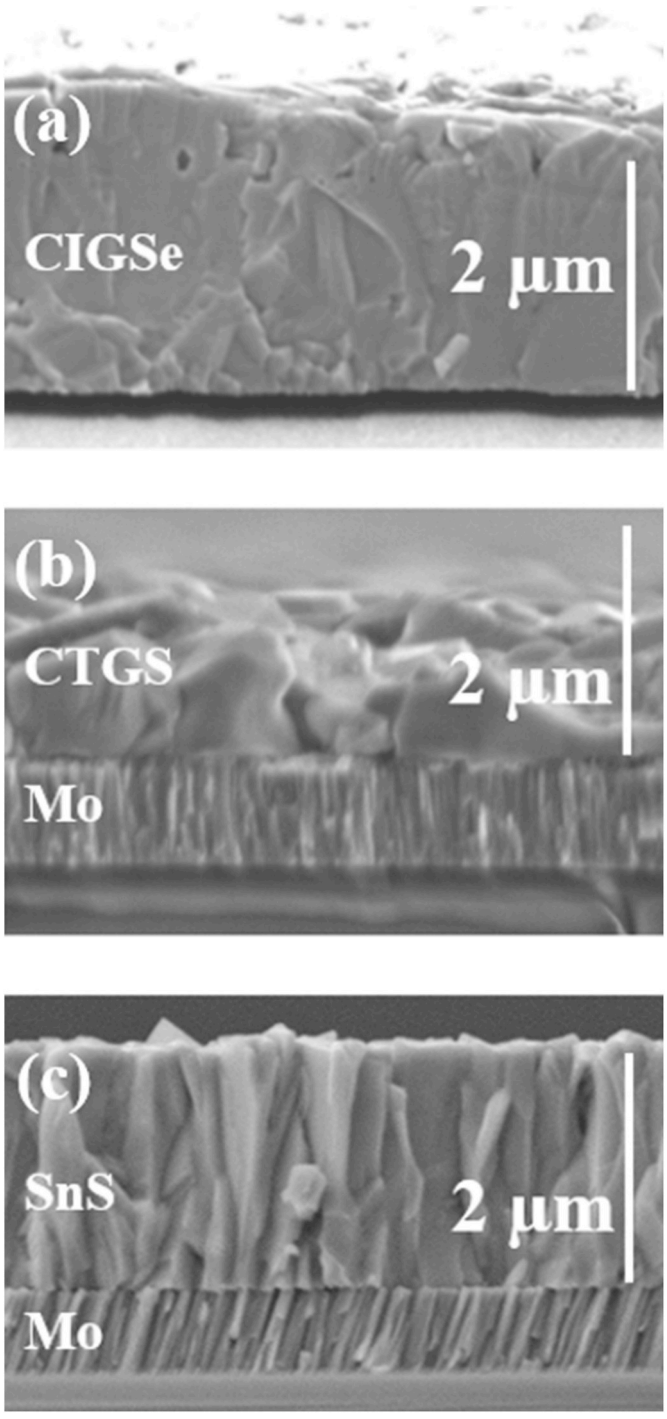

Fig. 3. Cross-sectional scanning-electron-microscopy images of (a) bare CIGSe, (b) CTGS, and (c) SnS thin films on the Mo-coated SLG substrates.

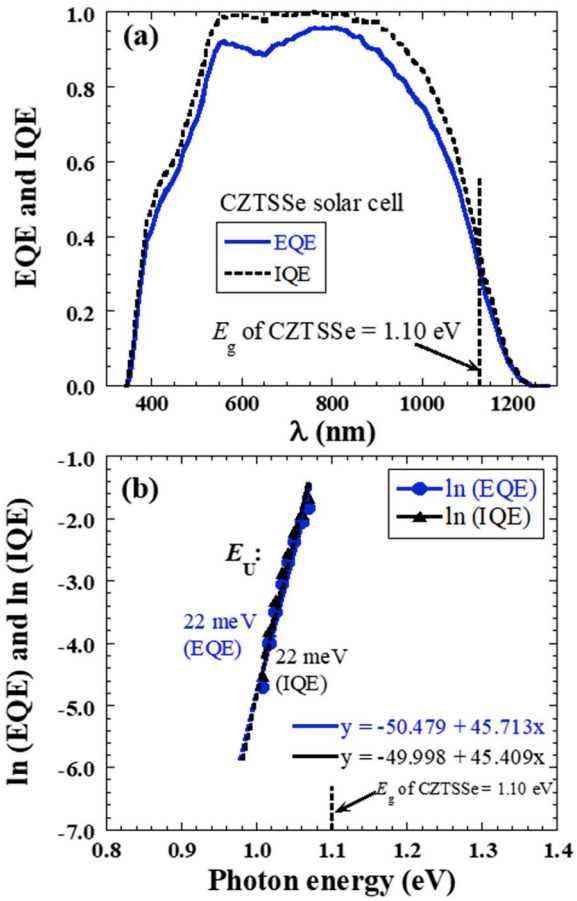

Fig. 4. (a) EQE and IQE spectra and (b) corresponding ln(EQE) and ln(IQE) in the long-wavelength edge (near the band edge) of the CZTSSe solar cell. The result of the CZTSSe solar cell was obtained from Ref. [29]. The λ denotes the wavelength.

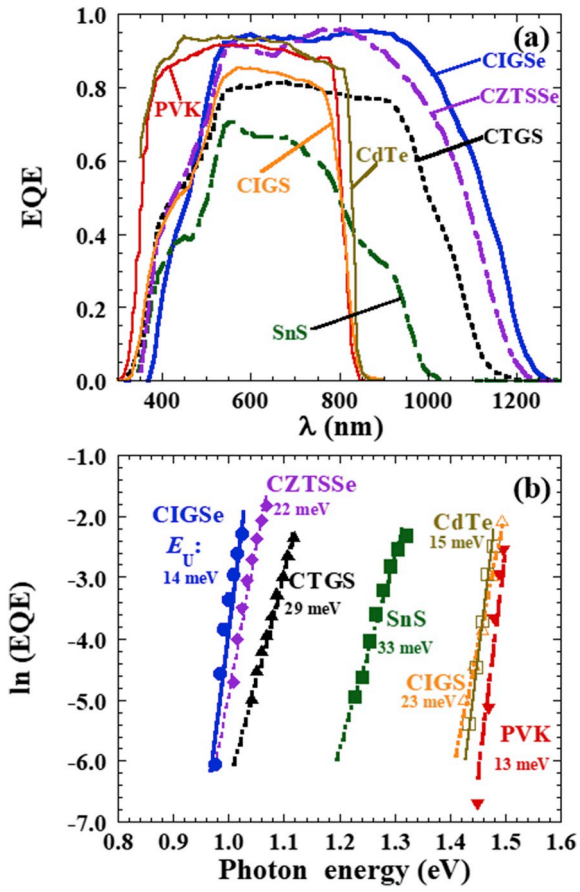

Fig. 5. (a) EQE spectra and (b) corresponding ln(EQE) in the long-wavelength edge (near the band edge) of the CIGSe, CZTSSe, CTGS, SnS, CIGS, PVK, and CdTe thin-film solar cells. The EQE spectra of the CIGSe, CZTSSe, CIGS, PVK and CdTe solar cells were obtained from Refs. [28–32]. The λ denotes the wavelength.

[24–26]. Therefore, the lowest J_0 for the CIGSe solar cells and the two highest J_0 for the CTGS and SnS solar cells are shown in Table 1. Fig. 3 additionally shows the cross-sectional scanning-electron-microscopy images of (a) bare CIGSe, (b) CTGS, and (c) SnS thin films, where the CIGSe thin film was deposited by multi-source evaporation, the CTGS thin film was prepared by the sulfurization of the stacked precursors of the Cu–SnS_2/Ge layers, and the SnS thin film was grown by the thermal evaporation. It is considered that the different grain sizes among the thin films are attributed to the different deposition process and method. The largest grains of the CIGSe thin film are shown, consistent with the lowest J_0 (the good quality of the absorber) for the CIGSe solar cell in Table 1, thus yielding the highest V_{OC} (the lowest $V_{OC,def}$) and *FF*. On the other the hand, the smaller grains of the CTGS and SnS thin films are demonstrated, corresponding to the higher J_0 values for the CTGS and SnS solar cell in Table 1, thus leading to lower V_{OC} (higher $V_{OC,def}$) and *FF*. According to the result, it is revealed that the quality (grain) of the thin-film absorber depending on the deposition process affects the cell performances especially V_{OC} and *FF* as well as the $V_{OC,def}$, and should have the impact on the tail absorption, characterized by the E_U. The correlations of the E_U values with the PV performances and $V_{OC,def}$ are interestingly investigated among the different types of thin-film solar cells.

3.2. Relations of E_U with photovoltaic performances and $V_{OC,def}$

The E_U values of the different types of thin-film solar cells were calculated. It has been reported that the E_U values of the absorbers of thin-films can be estimated from both their IQE and EQE in the long-wavelength edge [15–19]. The comparison of the E_U values estimated based on IQE and EQE is examined. Fig. 4 shows an example of (a) the EQE and IQE spectra and (b) corresponding ln(EQE) and ln(IQE) in the long-wavelength edge (near the band edge) of the CZTSSe solar cell with the E_g of 1.10 eV and cell performances shown in Table 1. The result of the CZTSSe solar cell was obtained from Ref. [29]. In Fig. 4(b), the inverse slopes of ln(EQE) and ln(IQE) in the long-wavelength edge (near the band edge (E_g of 1.10 eV)) with $h\nu$ yield the calculation of the E_U values. It is seen that the E_U values of 22 meV estimated based on the IQE and EQE spectra are similar in a long-wavelength edge, which is confirmed that the uses of EQE and IQE are justified to estimate the E_U.

The E_U values of the thin-film absorbers of the different-type thin-film solar cells were consequently calculated from their EQE spectra. Fig. 5 depicts (a) EQE spectra and (b) corresponding ln(EQE) in the long-wavelength edge (near the band edge) of the thin-film solar cells, which are the CIGSe, CZTSSe, CTGS, SnS, CIGS, PVK, and CdTe thin-film solar cells. The EQE spectra of the CIGSe, CZTSSe, CIGS, PVK, and CdTe solar cells were obtained from Refs. [28–32]. The E_U values of the different-type thin-film absorbers are estimated and shown in Fig. 5(b). The E_U values and photovoltaic performances of the CIGSe, CZTSSe, CTGS, and SnS solar cells are therefore presented in Table 1. It is demonstrated that the tail absorption characterized by the E_U has the significant impact on the cell performances and the J_0, where the lowest E_U value of 14 meV for the CIGSe solar cell demonstrates the lowest J_0 and the highest values of all cell performances with the η of 17.3% in Table 1.

The correlations of the E_U values with the PV performances of

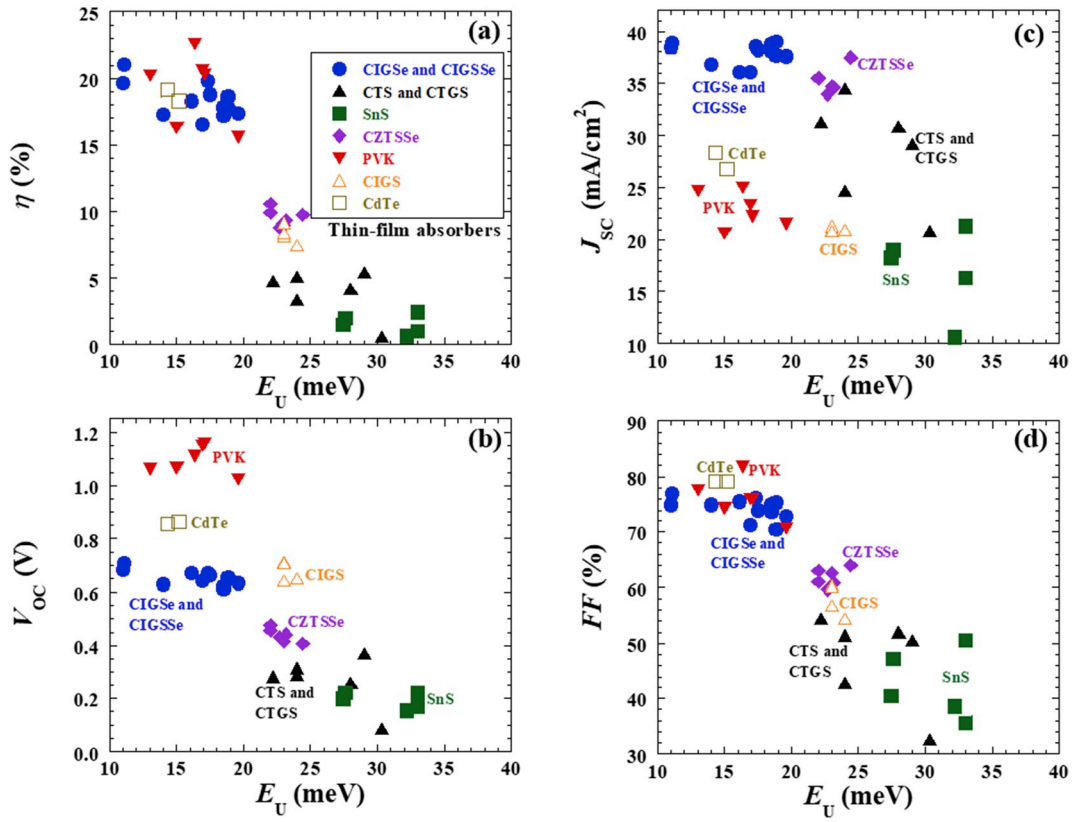

Fig. 6. PV performances (η, V_{OC}, J_{SC}, and *FF*) as a function of the E_U values of the thin-film absorbers of different-type thin-film solar cells, which are CIGSe, CIGSSe, CTS, CTGS, SnS, CZTSSe, PVK, CIGS, and CdTe thin-film solar cells. The cell performances and the E_U values were obtained and estimated based on the EQE spectra of the thin-film solar cells with the CIGSe and CIGSSe absorbers [28,33–35], the CZTSSe absorbers [29], the PVK absorbers [31,36–40], the CIGS absorbers [30], and the CdTe absorbers [32,41].

different-type thin-film solar cells are examined. Fig. 6 therefore shows PV performances (η, V_{OC}, J_{SC}, and *FF*) as a function of the E_U values of the thin-film absorbers of different-type thin-film solar cells, which are CIGSe, CIGSSe, CTS, CTGS, SnS, CZTSSe, PVK, CIGS, and CdTe thin-film solar cells. The cell performances and the E_U values were obtained and estimated based on the EQE spectra of the thin-film solar cells with the CIGSe and CIGSSe absorbers [28,33–35], the CZTSSe absorbers [29], the PVK absorbers [31,36–40], the CIGS absorbers [30], and the CdTe absorbers [32,41]. The estimated E_U values in Fig. 6 are well consistent with those reported by others [25,42]. It is determined that the relation between the J_{SC} and E_U of the thin-film solar cells is not clearly shown since the J_{SC} is mainly influenced by the E_g of the thin-film absorbers as previously explained. The low J_{SC} values are seen for the SnS, PVK, CIGS, and CdTe solar cells because the large E_g values of the SnS, PVK, CIGS, and CdTe absorbers are approximately 1.3, 1.5, 1.5, and 1.47 eV, respectively. Moreover, the large E_U values of over 20 meV are observed in cases of the CIGS, CTS, CTGS, SnS, and CZTSSe solar cells, thereby giving rise to low V_{OC} and *FF*. One of the explanations is that the CIGS thin films possess the small grains and very rough surface as reported in Ref. [9]. The CTS, CTGS, SnS thin films have the small grains in Fig. 3 and secondary phases both in their bulk and on their surface such as Sn_2S_3, SnS_2, CuS, SnS, and GeS phases for the CTS and CTGS films as well as Sn_2S_3 and SnS_2 phases for SnS film [43–45]. It has been furthermore reported that the dominant acceptors (Cu_{Zn}) in CZTS and CZTSSe have deeper ionization energy than that in V_{Cu} in CIGSe and CIGSSe, thereby resulting in the larger potential fluctuation in both conduction band and valence band [46]. The large density of the I-II antisite defects in the CZTSSe leads to the band tailing and the large deficit in cell performances [47–49]. Consequently, the higher E_U values (over 20 meV) for the CZTSSe than those for the CIGSe and CIGSSe are demonstrated with the lower V_{OC} and *FF*. As a result, the low η values of about 10% or lower for the CIGS, CTS, CTGS, SnS, and CZTSSe solar cells are shown with the large E_U values of over 20 meV. On the other hand, the low E_U values of below 20 meV for the CIGSe, CIGSSe, PVK, and CdTe solar cells give rise to the high η values, implying the high qualities of the CIGSe, CIGSSe, PVK, and CdTe thin films, which have been reported as their promising thin-film solar cells with the η of over 22% [50]. It has been reported that with the E_U above the k_BT the V_{OC} is strongly reduced [51],

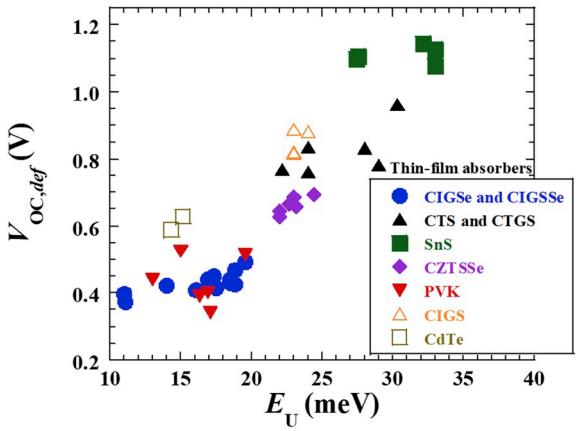

Fig. 7. $V_{OC,def}$ as a function of the E_U values of the thin-film absorbers of different-type thin-film solar cells, which are CIGSe, CIGSSe, CTS, CTGS, SnS, CZTSSe, PVK, CIGS, and CdTe thin-film solar cells. The $V_{OC,def}$ and the E_U values were obtained and estimated based on the EQE spectra of the thin-film solar cells with the CIGSe and CIGSSe absorbers [28,33–35], the CZTSSe absorbers [29], the PVK absorbers [31,36–40], the CIGS absorbers [30], and the CdTe absorbers [32,41].

attributable to the exponential increase in the J_0 [52], where the k_B and T denote Boltzmann constant and temperature. Therefore, one of the possible explanations is that the E_U values of below 20 meV are lower than thermal energy (k_BT) under room temperature (approximately 25 meV), possibly enhancing the carrier mobility and lifetime. According to the results, the E_U can be used as the indicator of the quality of the thin-film absorbers. The experimental results in this work are well consistent with the simulated result reported in Ref. [26], where it was theoretically described that the absorbers with the E_U values of below 20 meV is of important to realize high photovoltaic performances. Moreover, it has been experimentally reported that the E_U values of below 20 meV for the CIGSe solar cells lead to their high η (17–20.5%) [19].

It is known that the V_{OC} of the solar cells is also affected by the E_g of the absorbers. The relationship between the $V_{OC,def}$ and the E_U is therefore examined to exclude the effect of the E_g. It should be noted that the E_U values based on EQE are consistent with the E_U values based on photocurrent spectroscopy and photoluminescence [53]. Fig. 7 shows the corresponding $V_{OC,def}$ as a function of the E_U values of the thin-film absorbers of different-type thin-film solar cells, which are CIGSe, CIGSSe, CTS, CTGS, SnS, CZTSSe, PVK, CIGS, and CdTe thin-film solar cells. It is determined that the relationship between the $V_{OC,def}$ and the E_U was found, and the $V_{OC,def}$ is reduced with the decrease in the E_U, suggesting the improvement of the thin-film absorber quality as previously explained. According to the results, the E_U values of below 20 meV for the CIGSe, CIGSSe, PVK, and CdTe solar cell lead to the low $V_{OC,def}$ and high η values, whereas the E_U values of over 20 meV for the CIGS, CTS, CTGS, SnS, and CZTSSe solar cells give rise to the high $V_{OC,def}$ and the low η values. To further increase the η of the eco-friendly thin-film solar cells with earth-abundant elements such as CTS, CTGS, and SnS solar cells, their E_U values need to be reduced, i.e. lower than 20 meV, which could be done through further development of their deposition process.

4. Conclusions

In this contribution, the correlations of the E_U values with the PV performances and $V_{OC,def}$ were experimentally scrutinized and compared among the different types of thin-film solar cells. It is shown that the E_U values estimated based on the IQE and EQE spectra are similar in a long-wavelength edge. In addition, the relation between the J_{SC} and E_U of the thin-film solar cells is not clearly shown since the J_{SC} is mainly influenced by the E_g of the thin-film absorbers. On the other hand, the E_U has the significant impact on the V_{OC} (or $V_{OC,def}$) and *FF*, where the reduced E_U yields the increases in the V_{OC} (or reduced $V_{OC,def}$) and *FF*. The E_U can be therefore utilized as the index of the quality of the thin-film absorbers. The E_U values of over 20 meV, found in the CIGS, CTS, CTGS, SnS, and CZTSSe solar cells, give rise to the high $V_{OC,def}$ and the low η values. The E_U values of below 20 meV, which are observed in the CIGSe, CIGSSe, PVK, and CdTe solar cell, lead to the low $V_{OC,def}$ and high η values. This occurs because the E_U values of below 20 meV are lower than thermal energy under room temperature (approximately 25 meV), possibly decreasing the influence of the band tail states of the thin-films and enhancing the carrier mobility and lifetime. Ultimately, the thin-film absorbers with the E_U values of below 20 meV is of important to realize high PV performances.

CRediT authorship contribution statement

Jakapan Chantana: Conceptualization, Methodology, Formal analysis, Investigation, Resources, Writing - original draft, Writing - review & editing, Supervision, Data curation. **Yu Kawano:** Writing - review & editing. **Takahito Nishimura:** Writing - review & editing. **Abdurashid Mavlonov:** Writing - review & editing. **Takashi Minemoto:** Project administration, Writing - review & editing.

Acknowledgement

This work is partly supported by NEDO (the New Energy and Industrial Technology Development Organization) in Japan.

Appendix A. Supplementary data

Supplementary data to this article can be found online at https://doi.org/10.1016/j.solmat.2020.110502.

References

[1] Y. Hamakawa, Background and motivation for thin-film solar-cell development, in: Y. Hamakawa (Ed.), Thin-Film Solar Cells Next Generation Photovoltaics and its Applications, Springer, Heidelberg, 2004, pp. 1–14.
[2] E. Vallat-Sauvain, A. Shah, J. Bailat, Epitaxial thin film crystalline silicon solar cells on low cost silicon carriers, in: J. Poortmans, V. Arkhipov (Eds.), Thin Film Solar Cells, Fabrication, Characterization and Applications, Wiley, Chichester, 2006, pp. 1–32.
[3] P. Jackson, R. Wuerz, D. Hariskos, E. Lotter, W. Witte, M. Powalla, Effects of heavy alkali elements in Cu(In,Ga)Se_2 solar cells with efficiencies up to 22.6%, Phys. Status Solidi RRL 10 (2016) 583–586.
[4] M. Nakamura, K. Yamaguchi, Y. Kimoto, Y. Yasaki, T. Kato, H. Sugimoto, Cd-free Cu(In,Ga)$(S,Se)_2$ thin-film solar cell with record efficiency of 23.35%, IEEE J. Photovoltaics 9 (2019) 1863–1867.
[5] M.A. Green, E.D. Dunlop, J. Hohl-Ebinger, M. Yoshita, N. Kopidakis, A.W.Y. Ho-Baillie, Solar cell efficiency tables (Version 55), Prog. Photovoltaics Res. Appl. 28 (2020) 3–15.
[6] E.H. Jung, N.J. Jeon, E.Y. Park, C.S. Moon, T.J. Shin, T.-.Y. Yang, J.H. Noh, J. Seo, Efficiency, stable and scalable perovskite solar cells using poly(3-hexylthiophene), Nature 567 (2019) 511–515.
[7] P.M. Bridenbaugh, P. Migliorato, Junction electroluminescence in $CuInS_2$, Appl. Phys. Lett. 26 (1975) 459–460.
[8] J.L. Shay, P.M. Bridenbaugh, H.M. Kasper, Luminescent properties of $CuGaS_2$ doped with Cd or Zn, J. Appl. Phys. 45 (1974) 4491–4494.
[9] H. Hiroi, Y. Iwata, S. Adachi, H. Sugimoto, A. Yamada, New world-record efficiency for pure-sulfide Cu(In,Ga)S_2 thin-film solar cell with Cd-free buffer layer via KCN-free process, IEEE J. Photovoltaics 6 (2016) 760–763.
[10] H. Sugimoto, H. Hiroi, Y. Iwata, A. Yamada, Recent progress in high efficiency pure sulfide CIGS solar cells, in: Proceedings of the 27th International Photovoltaic Science and Engineering Conference, 2017.
[11] W. Wang, M.T. Winkler, O. Gunawan, T. Gokmen, T.K. Todorov, Y. Zhu, D.B. Mitzi, Device characteristics of CZTSSe thin-film solar cells with 12.6% efficiency, Adv. Energy Mater. 4 (2014) 1301465.
[12] M. Umehara, S. Tajima, Y. Aoki, Y. Takeda, T. Motohiro, $Cu_2Sn_{1-x}Ge_xS_3$ solar cells fabricated with a graded bandgap structure, APEX 9 (2016), 072301.
[13] J. Chantana, K. Tai, H. Hayashi, T. Nishimura, Y. Kawano, T. Minemoto, Investigation of carrier recombination of Na-doped Cu_2SnS_3 solar cell for its improved conversion efficiency of 5.1%, Sol. Energy Mater. Sol. Cells 2006 (2020) 110261.
[14] P. Sinsermsuksakul, L. Sun, S.W. Lee, H.H. Park, S.B. Kim, C. Yang, R.G. Gordon, Overcoming efficiency limitations of SnS-based solar cells, Adv. Energy Mater. 4 (2014) 1400496.
[15] J. Mattheis, P.J. Rostan, U. Rau, J.H. Werner, Carrier collection in Cu(In,Ga)Se_2 solar cells with graded band gaps and transparent ZnO:Al back contacts, Sol. Energy Mater. Sol. Cells 91 (2007) 689–695.
[16] M. Troviano, K. Taretto, Urbach Energy in CIGS extracted from quantum efficiency analysis of high performance CIGS solar cells, In 24th European Photovoltaic Solar Energy Conference (Hamberg) 2009 2933.
[17] M. Troviano, K. Taretto, Analysis of internal quantum efficiency in double-graded bandgap solar cells including sub-bandgap absorption, Sol. Energy Mater. Sol. Cells 95 (2011) 821–828.
[18] J. Chantana, Y. Kawano, T. Nishimura, T. Minemoto, Urbach energy of Cu(In,Ga)Se_2 and Cu(In,Ga)$(S,Se)_2$ absorbers prepared by various methods: indicator of their quality, Mater. Today Commun. 21 (2019) 100652.
[19] R. Carron, S. Nishiwaki, T. Thomas, T. Feurer, R. Hertwig, E. Avancini, J. Lockinger, S.-C. Yang, S. Buecheler, A.N. Tiwari, Advanced Alkali treatments for high-efficiency Cu(In,Ga)Se_2 solar cells on flexible substrates, Adv. Energy Mater. 9 (2019) 1900408.
[20] J.A. Schmidt, M. Hundhausen, L. Ley, Transport properties of a-$Si_{1-x}C_x$: H films investigated by the moving photocarrier grating technique, Phys. Rev. B 62 (2000) 13010–13015.
[21] R. Braunstein, Y. Tang, S. Dong, J. Liebe, G. Sun, A. Kattwinkel, Photocharge Transport and Recombination Measurements in Amorphous Silicon Films and Solar Cells by Photoconductive Frequency Mixing, Subcontractor Report, 1999. NREL/SR-520-26127.
[22] J. Chantana, T. Kato, H. Sugimoto, T. Minemoto, Investigation of correlation between open-Circuit voltage deficit and carrier recombination rates in Cu(In,Ga)$(S,Se)_2$-based thin-film solar cells, Appl. Phys. Lett. 112 (2018) 151601.
[23] J.V. Li, S. Grover, M.A. Contreras, K. Ramanathan, D. Kuciauskas, R. Noufi, A recombination analysis of Cu(In,Ga)Se_2 solar cells with low and high Ga composition, Sol. Energy Mater. Sol. Cells 124 (2014) 143–149.

[24] U. Rau, B. Blank, T.C.M. Muller, T. Kirchartz, Efficiency potential of photovoltaic materials and devices unveiled by detailed-balance analysis, Phys. Rev. Appl. 7 (2017), 044016.

[25] S.D. Wolf, J. Holovsky, S.-J. Moon, P. Loper, B. Niesen, M. Ledinsky, F.-J. Haug, J.-H. Yum, C. Ballif, Organometallic halide perovskites: sharp optical absorption edge and its relation to photovoltaic performance, J. Phys. Chem. Lett. 5 (2014) 1035–1039.

[26] Y. Kato, S. Fujimoto, M. Kozawa, H. Fujiwara, Maximum efficiencies and performance-limiting factors of inorganic and hybrid perovskite solar cells, Phys. Rev. Appl. 12 (2019), 024039.

[27] Y. Kawano, J. Chantana, T. Minemoto, Impact of growth temperature on the properties of SnS film prepared by thermal evaporation and its photovoltaic performance, Curr. Appl. Phys. 15 (2015) 897–901.

[28] J. Chantana, S. Teraji, T. Watanabe, T. Minemoto, Influences of Fe and absorber thickness on photovoltaic performances of flexible Cu(In,Ga)Se_2 solar cell on stainless steel substrate, Sol. Energy 173 (2018) 126–131.

[29] D. Hironiwa, J. Chantana, N. Sakai, T. Kato, H. Sugimoto, T. Minemoto, Application of multi-buffer layer of (Zn,Mg)O/CdS in $Cu_2ZnSn(S,Se)_4$ solar cells, Curr. Appl. Phys. 15 (2015) 383–388.

[30] T. Nishimura, S. Kim, J. Chantana, Y. Kawano, S. Ishizuka, T. Minemoto, Application of Al-doped (Zn,Mg)O on pure-sulfide Cu(In,Ga)S_2 solar cells for enhancement of open-circuit voltage, Sol. Energy Mater. Sol. Cells 202 (2019) 110157.

[31] W.S. Yang, J.H. Noh, N.J. Jeon, Y.C. Kim, S. Ryu, J. Seo, S.I. Seok, High-performance photovoltaic perovskite layers fabricated through intramolecular exchange, Science 348 (2015) 1234–1237.

[32] J. Sites, A. Munshi, J. Kephart, D. Swanson, W.S. Sampath, Progress and challenges with CdTe cell efficiency, in: IEEE 43rd Photovoltaic Specialists Conference, Portland, OR, USA, 2016, pp. 3632–3635, https://doi.org/10.1109/PVSC.2016.7750351.

[33] J. Chantana, T. Kato, H. Sugimoto, T. Minemoto, Heterointerface recombination of Cu(In,Ga)(S,Se)$_2$-based solar cells with different buffer layers, Prog. Photovoltaics Res. Appl. 26 (2018) 127–134.

[34] J. Chantana, T. Kato, H. Sugimoto, T. Minemoto, Enhancement of photovoltaic performances of Cu(In,Ga)(S,Se)$_2$ solar cell through combination of heat-light soaking and light soaking processes, Prog. Photovoltaics Res. Appl. (2018), https://doi.org/10.1002/pip.3031.

[35] T. Nishimura, H. Sugiura, K. Nakada, A. Yamada, Accurate control and characterization of Cu depletion layer for highly efficient Cu(In,Ga)Se_2 solar cells, Prog. Photovoltaics Res. Appl. 27 (2019) 171–178.

[36] N.J. Jeon, J.H. Noh, Y.C. Kim, W.S. Yang, S. Ryu, S.I. Seok, Solvent engineering for high-performance inorganic-organic hybrid perovskite solar cells, Nat. Mater. 13 (2014) 897–903.

[37] W. Chen, Y. Wu, Y. Yue, J. Liu, W. Zhang, X. Yang, H. Chen, E. Bi, I. Ashraful, M. Gratzel, L. Han, Efficient and stable large-area perovskite solar cells with inorganic charge extraction layers, Science 350 (2015) 944–948.

[38] C. Yi, J. Luo, S. Meloni, A. Boziki, N. Ashari-Astani, C. Gratzel, S.M. Zakeeruddin, U. Rothlisberger, M. Gratzel, Entropic stabilization of mixed A-cation ABX_3 metal halide perovskites for high performance perovskite solar cells, Energy Environ. Sci. 9 (2016) 656–662.

[39] M.M. Lee, J. Teuscher, T. Miyasaka, T.N. Murakami, H.J. Snaith, Efficient hybrid solar cells based on meso-superstructured organometal halide perovskites, Science 338 (2012) 643–647.

[40] J.H. Heo, S.H. Im, J.H. Noh, T.N. Mandal, C.-S. Lim, J.A. Chang, Y.H. Lee, H. Kim, A. Sarkar, Md K. Nazeeruddin, M. Gratzel, S.I. Seok, Efficient inorganic-organic hybrid heterojunction solar cells containing perovskite compound and polymeric hole conductors, Nat. Photon. 7 (2013) 486–491.

[41] A.H. Munshi, J. Kephart, A. Abbas, J. Raguse, J.-N. Beaudry, K. Barth, J. Sites, J. Walls, W. Sampath, Polycrystalline CdSeTe/CdTe absorber cells with 28 mA/cm^2 short-circuit current, IEEE J. Photovoltaics 8 (2018) 310–314.

[42] C.M. Sutter-Fella, D.W. Miller, Q.P. Ngo, E.T. Roe, F.M. Toma, I.D. Sharp, M. C. Lonergan, A. Javey, Band tailing and deep defect states in $CH_3NH_3Pb(I_{1-x}Br_x)_3$ perovskites as revealed by sub-bandgap photocurrent, ACS Energy Lett. 2 (2017) 709–715.

[43] K. Suzuki, J. Chantana, T. Minemoto, Na role during sulfurization of NaF/Cu/SnS_2 stacked precursor for formation of Cu_2SnS_3 thin film as absorber of solar cell, Appl. Surf. Sci. 414 (2017) 140–146.

[44] K. Hamamura, J. Chantana, K. Suzuki, T. Minemoto, Influence of Cu/(Ge + Sn) composition ratio on photovoltaic performances of $Cu_2Sn_{1-x}Ge_xS_3$ solar cell, Sol. Energy 149 (2017) 341–346.

[45] Y. Kawano, Y. Kodani, J. Chantana, T. Minemoto, Effects of Na and secondary phases on physical properties of SnS thin film after sulfurization process, Jpn. J. Appl. Phys. 55 (2016), 092301.

[46] L. Yin, G. Cheng, Y. Feng, Z. Li, C. Yang, X. Xiao, Limitation factors for the performance of kesterite Cu_2ZnSnS_4 thin film solar cells studied by defect characterization, RSC Adv. 5 (2015) 40369.

[47] B.G. Mendis, M.D. Shannon, M.C.J. Goodman, J.D. Major, R. Claridge, D. P. Halliday, K. Durose, Direct observation of Cu, Zn cation disorder in Cu_2ZnSnS_4 solar cell absorber material using aberration corrected scanning transmission electron microscopy, Prog. Photovoltaics Res. Appl. 22 (2014) 24–34.

[48] T. Gershon, B. Shin, T. Gokmen, S. Lu, N. Bojarczuk, S. Guha, Relationship between Cu_2ZnSnS_4 quasi donor-acceptor pair density and solar cell efficiency, Appl. Phys. Lett. 103 (2013) 193903.

[49] T. Gershon, K. Sardashti, O. Gunawan, R. Mankad, S. Singh, Y.S. Lee, J.A. Ott, A. Kummel, R. Haight, Photovoltaic device with over 5% efficiency based on an n-type Ag_2ZnSnS_4 absorber, Adv. Energy Mater. 6 (2016) 1601182.

[50] M. Powalla, S. Paetel, E. Ahlswede, R. Wuerz, C.D. Wessendorf, T.M. Friedlmeier, Thin-film solar cells exceeding 22% solar cell efficiency: an overview on CdTe-, Cu(In,Ga)Se_2-, and perovskite-based materials, Appl. Phys. Rev. 2 (2018), 041602.

[51] J. Jean, T.S. Mahony, D. Bozyigit, M. Sponseller, J. Holovsky, M.G. Bawendi, V. Bulovic, Radiative efficiency limit with band tailing exceeds 30% for quantum dot solar cells, ACS Energy Lett. 2 (2017) 2616–2624.

[52] K. Tanaka, T. Minemoto, H. Takakura, Analysis of heterointerface recombination by $Zn_{1-x}Mg_xO$ for window layer of Cu(In,Ga)Se_2 solar cells, Sol. Energy 83 (2009) 477–479.

[53] S. Siebentritt, E. Avancini, M. Bar, J. Bombsch, E. Bourgeois, S. Buecheler, R. Carron, C. Castro, S. Duguay, R. Felix, E. Handick, D. Hariskos, V. Havu, P. Jackson, H.-P. Komsa, T. Kunze, M. Malitckaya, R. Menozzi, M. Nesladek, N. Nicoara, M. Puska, M. Raghuwanshi, P. Pareige, S. Sadewasser, G. Sozzi, A. N. Tiwari, S. Ueda, A. Vilalta-Clemente, T.P. Weiss, F. Werner, R.G. Wilks, W. Witte, M.H. Wolter, Adv. Energy Mater. (2020) 1903752, https://doi.org/10.1002/aenm.201903752.